Tensile Crack Modeling Cohesive Slopes and Vertical Cuts

M. Rezaiee-Pajand[i]; M. Moayyedian[i]; F. Molaee[i]

ABSTRACT

In order to improve the analysis of cohesive slopes and vertical cuts, tensile crack modeling is used. Nonlinear elasto-plastic finite element analysis along with Mohr-Coloumb yield surface and associated flow rule have been utilized. Both formulations and numerical examples are presented in this paper. The results of test problems reveal that tensile cracks will reduce the factor of safety. This reduction is more pronounced when the soil slope gets steeper.

KEYWORDS

Slopes, Vertical cut, Nonlinear analysis, Finite element, Tensile crack, Elasto-plastic, Mohr-Coloumb

INTRODUCTION

If a tensile stress occurs in a tension week material, the body will crack. Although crack modeling has been performed in concrete, steel and ceramic materials, this property has not been distinguished in soil structures. The reason is the difficulty in soil crack modeling. Slope and vertical cut analysis shows great tensile stresses. However, in the finite element slope stability analysis, tensile cracks are not considered [1]. Neglecting the cracks, the material can only behave elastic-plastic. Many different methods have been used for crack modeling being smeared crack, discrete crack, interface crack and fracture mechanics modeling.

SMEARED CRACK MODELING

A simple and yet convenient method for crack modeling is smeared crack. In this method, the cracks are assumed to be distributed in the element [2,3]. When the principal tensile stress is greater than the tensile strength of material, a crack is formed[i]. Figure 1 shows a body cracked in the x' direction. In this figure, ψ is the angle between the crack direction and the x axis.

After a crack has occurred, material will behave orthotropically. The material matrix and stress vector should be modified after cracking. For plane stress conditions, the stress - strain relations after cracking can be written as:

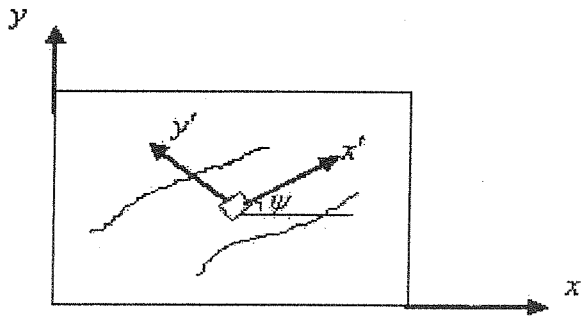

Figure 1: Crack formation

$$\begin{Bmatrix} d\sigma_{x'} \\ d\sigma_{y'} \\ d\tau_{x'y'} \end{Bmatrix} = \begin{bmatrix} E & 0 & 0 \\ 0 & 0 & 0 \\ 0 & 0 & 0 \end{bmatrix} \begin{Bmatrix} d\varepsilon_{x'} \\ d\varepsilon_{y'} \\ d\gamma_{x'y'} \end{Bmatrix} \tag{1}$$

For plane strain, $E/(1-\nu^2)$ is used instead of E in Eq (1). Therefore, the equation is generally written as:

$$\{\Delta\sigma\} = [D_{cr}]_c \{\Delta\varepsilon\} \tag{2}$$

Here, $[D_{cr}]_c$ is the cracked material matrix. This matrix can not model real material behavior exactly, because, when the crack width is small some shear stress can be transferred. So, equation (1) is modified as:

$$\begin{Bmatrix} d\sigma_{x'} \\ d\sigma_{y'} \\ d\tau_{x'y'} \end{Bmatrix} = \begin{bmatrix} E & 0 & 0 \\ 0 & 0 & 0 \\ 0 & 0 & \beta_t G \end{bmatrix} \begin{Bmatrix} d\varepsilon_{x'} \\ d\varepsilon_{y'} \\ d\gamma_{x'y'} \end{Bmatrix} \tag{3}$$

The β_t factor equals 1 in the crack initiation phase. By widening the crack width, β_t goes toward 0. If β_t equals 1, the material matrix will be isotropic. In this paper, β_t is assumed to be equal to 0.1.

If a second crack is formed, the constitutive relation should be written as:

$$\begin{Bmatrix} d\sigma_{x'} \\ d\sigma_{y'} \\ d\tau_{x'y'} \end{Bmatrix} = \begin{bmatrix} 0 & 0 & 0 \\ 0 & 0 & 0 \\ 0 & 0 & \beta_t G \end{bmatrix} \begin{Bmatrix} d\varepsilon_{x'} \\ d\varepsilon_{y'} \\ d\gamma_{x'y'} \end{Bmatrix} \tag{4}$$

In the finite element analysis, the material matrix should be transformed from crack axes (x' and y') to element local axes (x and y). This transformation is performed using:

$$[D_{cr}]_l = [T]^T [D_{cr}]_c [T] \tag{5}$$

[i] Department of Civil Engineering, Ferdowsi University of Mashhad, Iran. mrpajand@yahoo.com.

Here, $[D_{cr}]_c$ and $[D_{cr}]_l$ are material matrices in crack and local axes, respectively. The transformation matrix is written as[4-6]:

$$[T]=\begin{bmatrix} \cos^2\psi & \sin^2\psi & \sin\psi\cos\psi \\ \sin^2\psi & \cos^2\psi & -\sin\psi\cos\psi \\ -2\sin\psi\cos\psi & 2\sin\psi\cos\psi & \cos^2\psi-\sin^2\psi \end{bmatrix} \quad (6)$$

If one assumes $c=\cos\psi$ and $s=\sin\psi$, the cracked material matrix in local axes, for the first crack formation, can be found as:

$$[D_{cr}]=\begin{bmatrix} c^4E+4c^2s^2\beta_tG & c^2s^2E+4c^2s^2\beta_tG & c^3s\ E+2cs(c^2-s^2)\beta_tG \\ c^2s^2E+4c^2s^2\beta_tG & s^4E+4c^2s^2\beta_tG & c\ s^3E+2cs(c^2-s^2)\beta_tG \\ c^3s\ E+2cs(c^2-s^2)\beta_tG & c\ s^3E+2cs(c^2-s^2)\beta_tG & c^2s^2E+(c^2-s^2)\beta_tG \end{bmatrix} \quad (7)$$

. For crack formation in two perpendicular directions, the material matrix is written as:

$$[D_{cr}]=\begin{bmatrix} 4c^2s^2\beta_tG & 4c^2s^2\beta_tG & 2cs(c^2-s^2)\beta_tG \\ 4c^2s^2\beta_tG & 4c^2s^2\beta_tG & 2cs(c^2-s^2)\beta_tG \\ 2cs(c^2-s^2)\beta_tG & 2cs(c^2-s^2)\beta_tG & (c^2-s^2)\beta_tG \end{bmatrix} \quad (8)$$

The stresses should be corrected after crack has occurred. If $\sigma_{y'}$ and $\tau_{x'y'}$ are assumed to become zero after the first crack formation, the released stresses in the $x'y'$ coordinates can be found by:

$$\{\sigma'\}_{rel}=\{\sigma_{x'} \quad \sigma_{y'} \quad \tau_{x'y'}\}^T-\{\sigma_{x'} \quad 0 \quad 0\}^T \quad (9)$$

The released stress vector in local element coordinates can be written as:

$$\{\sigma\}_{rel}=\{\sigma_x \quad \sigma_y \quad \tau_{xy}\}^T-\{b(\psi)\}\sigma_{x'} \quad (10)$$

The transformation vector, $b(\psi)$, is given by:

$$b(\psi)=\{c^2 \quad s^2 \quad cs\}^T \quad (11)$$

On the other hand, $\sigma_{x'}$ can be written as a function of σ_x, σ_y and τ_{xy} as:

$$\sigma_{x'}=\{b'(\psi)\}^T\{\sigma_x \quad \sigma_y \quad \tau_{xy}\}^T \quad (12)$$

$$b'(\psi)=\{c^2 \quad s^2 \quad 2cs\}^T \quad (13)$$

Based upon these, the released stress in the element local coordinates can be written as:

$$\{\sigma\}_{rel}=([I]-\{b(\psi)\}\{b'(\psi)\}^T)\{\sigma_x \quad \sigma_y \quad \tau_{xy}\}^T \quad (14)$$

Here, $[I]$ is the unity matrix. It should be mentioned that Equation (14) can be abbreviated as:

$$\{\sigma\}_{rel}=[r]\{\sigma\} \quad (15)$$

$$[r]=\begin{bmatrix} 1-c^4 & -c^2s^2 & -2c^3s \\ -c^2s^2 & 1-s^4 & -2cs \\ -c^3s & -cs^3 & 1-2c^2s^2 \end{bmatrix} \quad (16)$$

Because of stress redistribution, some cracks may close. The crack closing criteria can be the return of strain to the first cracking strain, which is not conservative. In this paper, it is assumed that when the strain at a point becomes zero, the crack is closed. After the crack is closed, compressive stress can be transferred across the precracked zone. On the other hand, shear stress transfer will not be completely possible as before. So, the shear modulus should be modified as β_cG. The β_c factor is assumed to be equal to 0.9.

TENSILE STRENGTH OF SOILS

There is a little data about tensile strength of soils. One of the main reasons is the difference in the results of tests. Bishop and Garga has investigated the tensile strength of London clays in drained conditions. They found that the tensile stress of that kind of soil is consistent with the equation suggested by Hook [7]:

$$\sigma_c=-\frac{4\sigma_t}{\sqrt{1+\mu^2}-\mu} \quad (17)$$

Here, σ_c and σ_t are the drained unconfined compressive and tensile strengths of the soil, respectively. Also, μ is the tangent of friction angle across microcracks. Skampton has suggested a value between tan(18.5) and tan(30) for this parameter.

Based on these values, the ratio σ_t/σ_c can be found to be between 0.144 and 0.178. It should be added that many experiemtal methods have been proposed to find the tensile strength of soils [7,8].

SLOPE STABILITY FACTOR OF SAFETY

To use the finite element analysis for finding the factor of safety of slopes, a computer program has been written considering elasto-plastic and crack behavior of cohesive soils. The Mohr – Coloumb failure criteria has been used for elasto-plastic analysis and the cracks are modeled using smeared crack method [9,10]. It is assumed that after cracking the stress normal to the crack becomes zero immediately. In other words, strain softening is not considered [5].

The eight node isoparametric plane strain elements is used for the analysis. The stresses are found in Gauss points and if the principal tensile stress is greater than the tensile strength of the soil, a crack is assumed in that point. Otherwise, Mohr – Coloumb criteria is controlled for checking elasto-plastic behavior. The residual load is computed and analysis will be repeated.

To find the factor of safety, the soil parameters, being cohesion and tensile strength, are divided by assumed factors. These parameters will be:

$$c_f = \frac{c}{FOS} \quad , \quad T_f = \frac{T}{FOS} \tag{18}$$

When the number of iterations for convergence or the maximum displacement has a sudden change for a specific *FOS*, that would be the factor of safety of the structure [1,6].

NUMERICAL EXAMPLES

In order to show the performance of the method, a number of examples has been solved. The results are given in this paper. The numerical examples show that tensile cracks will reduce the factor of safety (*FOS*).

NONSTEEP SLOPE

A slope shown in Figure 2 is considered. For modeling of the slope 800 eight noded isoparametric elements have been used. The soil properties are as follows:

$C = 5$ KN/m^2
$\gamma = 20$ KN/m^3
$E = 10^5$ KN/m^2
$\nu = 0.3$

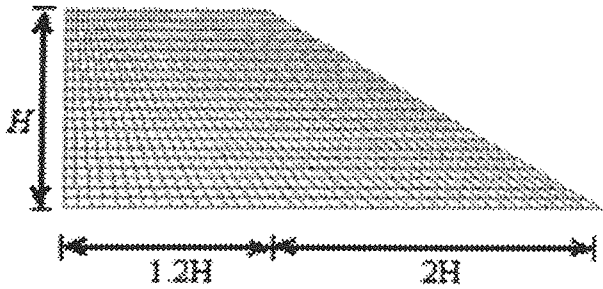

Figure 2: Nonsteep slope

If the tensile cracks are ignored, the *FOS* using Bishop and finite element methods will be equal to 2.03 and 2.06, respectively. Figure 3 shows the failure circle and Figure 4 shows the deformed finite element mesh using elasto-plastic constitutive relations. Comparing these figures, their consistency can be found.

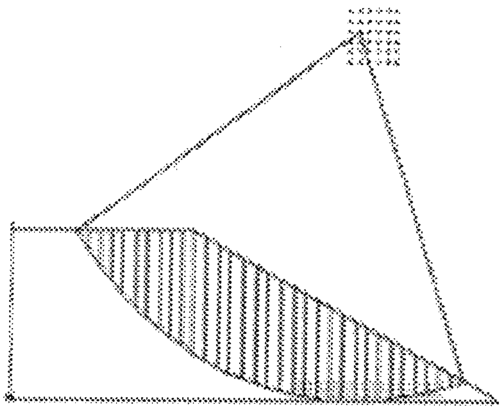
Figure 3: Failure circle

Considering the tensile cracks, using tensile strength of the soil equal to 5 percent of unconfined compressive strength (0.5 KN/m^2), the *FOS* will be found to be equal to 1.94.

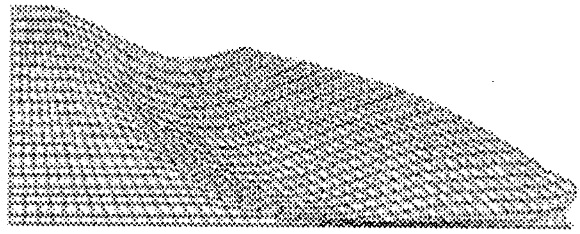
Figure 4: Elasto-Plastic deformation

This means 5.8 percent reduction in *FOS*. It should be noted that a little tensile stresses happen in this slope. Figure 5 shows the deformed shape considering cracks. It is clear that in some elements, in the upper zone of the slope, the cracks are formed. Using smaller tensile strength the cracks will propagate to other elements.

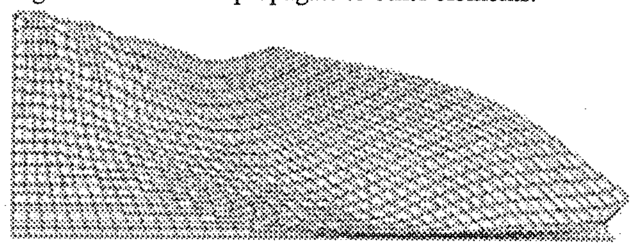
Figure 5: Cracked deformation

STEEP SLOPE

Figure 6 shows the slope analyzed in this example, which is much steeper than the previous one. The soil properties are the same as previous example.

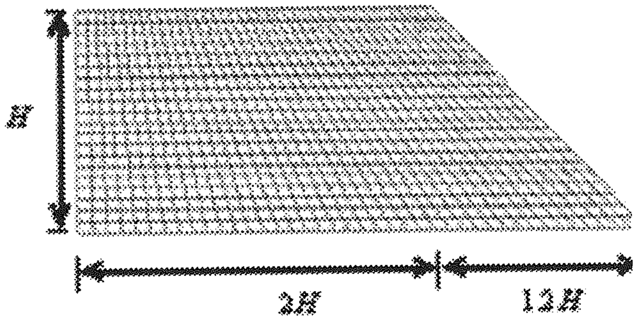

Figure 6: Steep slope

Bishop assumption and finite element elasto-plastic analysis will lead to a FOS equal to 1.63 and 1.66, respectively. Considering tensile cracks in the analysis will reduce FOS about 7.83 percent when using tensile strength equal to 5 percent of unconfined compressive strength. Figures 7 and 8 show the deformed shape neglecting and considering cracks, respectively.

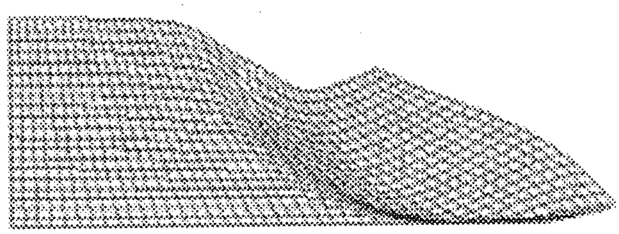

Figure 7: Elasto- plastic deformed shape

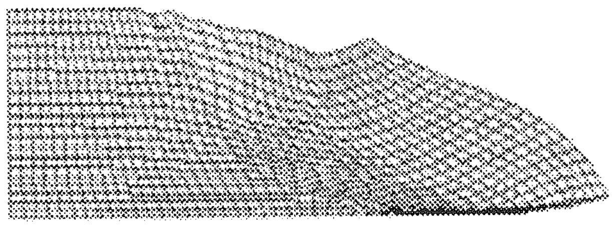

Figure 8: Cracked deformation

Using higher tensile strength will lead to higher factors of safety. Figure 9 shows the relationship between tensile strength and FOS for this example and the previous one. It can be found that as the slope gets steeper, the tensile cracks will have more influence on the factor of safety.

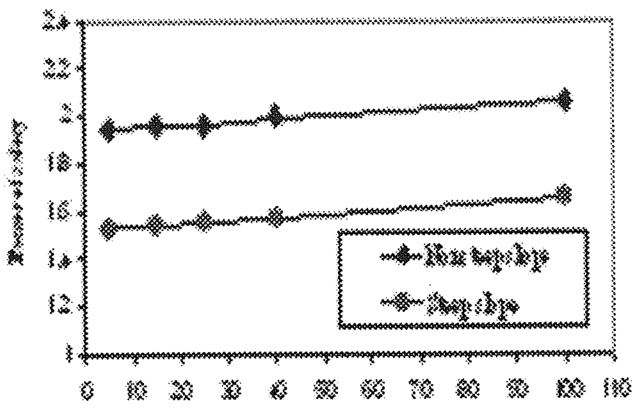

Ratio of tension resistance and unconfined compression resistance in percent

Figure 9: FOS variations in slopes

SHALLOW VERTICAL CUT

A vertical cut in $8H$ height cohesive soil, as shown in Figure (10), is considered. The soil properties are as follows:

$C = 90$ KN/m^2

$\gamma = 19$ KN/m^3

$E = 1.5*10^5$ KN/m^2

$\nu = 0.3$

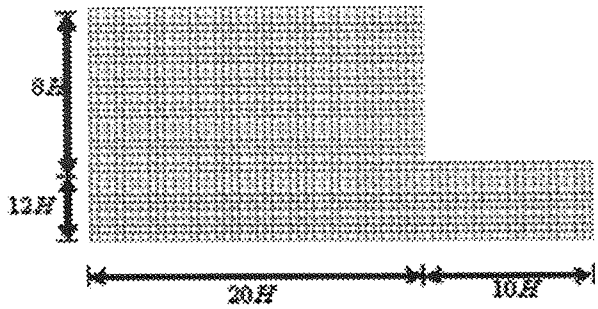

Figure 10 Shallow vertical cut

The slope is analyzed utilizing 1400 elements. Using the finite element method and Mohr – Coloumb criteria, neglecting tensile cracks, the factor of safety will be found to be equal to 2.38. The deformed shape is shown in Figure 11.

Assuming tensile strength of soil equal to 5, 15, 25and 40 percent of its compressive strength will lead to FOS equal to 1.51, 1.69, 1.81 and 2.03, respectively. This means 29 percent reduction in FOS, for σ_t/σ_c=0.15. Figure 12 shows the crack initiation and propagation. It can be found that in upper regions cracks are formed, and in the toe, elasto-plastic failure occurs.

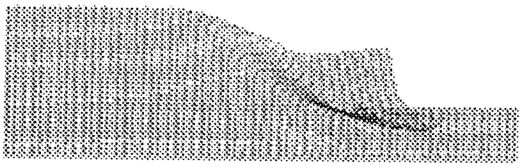

Figure 11 Elasto- plastic deformation

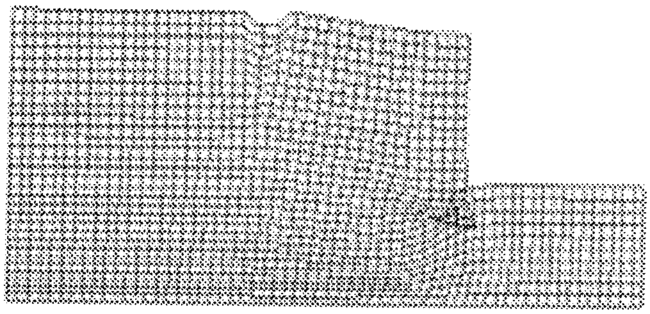

Figure 12 Cracked deformed shape

DEEP VERTICAL CUT

In this example the vertical cut height of the previous example is assumed to be equal to $12H$. Using elasto-plastic finite element analysis, the factor of safety is found to be equal to 1.58. The deformed shape in this analysis is shown in figure 13.

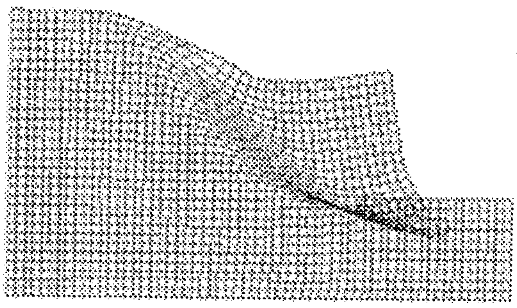

Figure 13 Deformed shape by elasto-plastic analysis

Elasto-plastic cracked finite element analysis with tensile strength equal to 5,15,25 and 40 percent of compressive
strength of soil leads to FOS equal to 0.89, 1.12, 1.22 and 1.32, respectively. Figure 14 shows the deformed shape in this type of analysis.

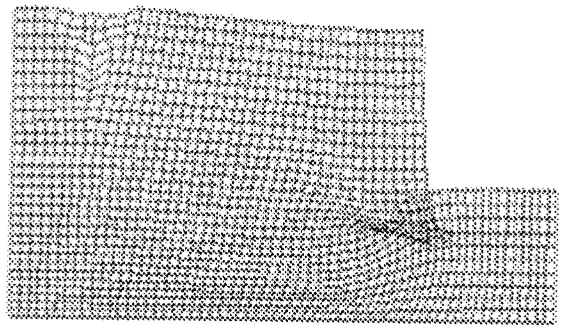

Figure 14 Cracked deformed shape

In figure 15, the relationship between tensile strength and factor of safety for the two last examples is shown. It is evident that tensile cracks Influence *FOS* significantly in vertical cuts.

CONCLUSION

To find the factor of safety of soil slopes and vertical cuts, nonlinear elasto-plastic finite element analysis using Mohr – Coloumb yield surface and associated flow rule have been used. Furthermore, the tensile cracks in these structures have been modeled using smeared crack method. The numerical examples show that tensile cracks will reduce the factor of safety. Also, the tensile cracks will have more influence on the factor of safety as the soil slope gets steeper or the tensile strength of the soil is decreased. This reduction will be the largest in vertical cuts. Based upon these facts, it is proposed that tensile cracks should be considered in steep soil slopes.

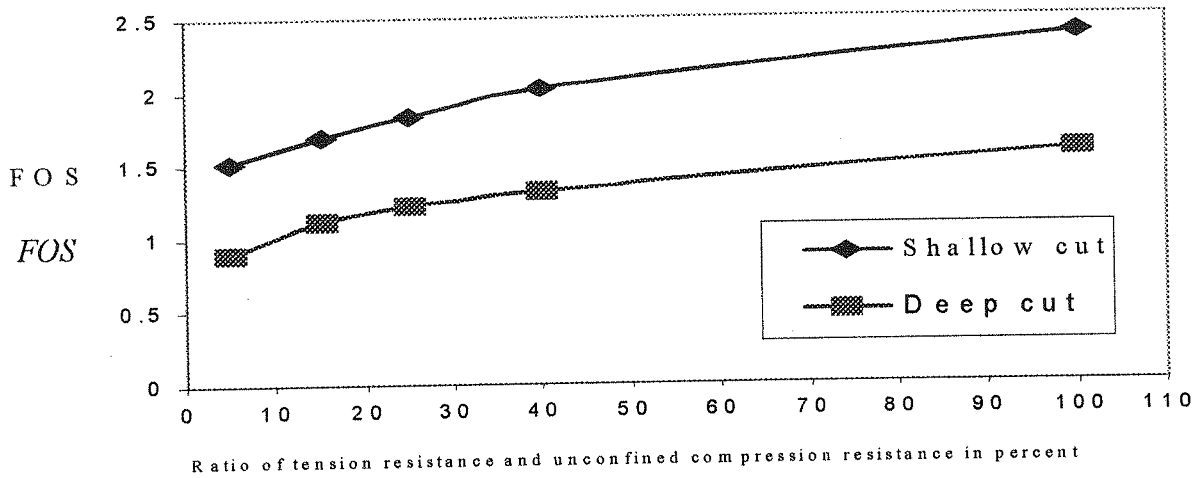

Figure 15 *FOS* variations in vertical cuts

REFERENCES

[1] Griffiths,D.V., and Lane,P.A., "Slope Stability Analysis by Finite Elements", Geotechnique , Vol. 49 ,PP. 387-403,(1999)

[2] Chen,W.F., Plasticity in Reinforced Concrete, McGraw-Hill Book Company, (1982).

[3] Lotfi,H.R., and Shing,B., " An Interface Model Applied to Fracture of Masonry Structures", Journal of the Structural Engineering, ASCE, Vol.120, No.1, PP.63-80 (1995)

[4] Cedolin,L., Darwin,D., Ingraffea,A.R., Pecknold,E.A., and Schnobrich,W.C., "Concrete Cracking", Finite Element Analysis of Reinforced Concrete, ASCE, New York, (1982)

[5] Kotsovos,M.D., and Pavlovich,M.N., Structural Concrete, Finite Element Analysis for Limit State Design, Thomas Telford, (1995)

[6] Hinton,E., Numerical Methods and Software for Dynamic Analysis of Plates and Shells, Pineridge Press, PP. 357-358, (1988)

[7] Lane,P.A., Griffiths,D.V., "Assessment of Stability of Slopes Under Drawdown Condition" , Jornal of Geotechnical Engineering, ASCE, Vol. 126, No. 5, PP. 443-450, (2000)

[8] Bishop,A.W., and Garga,V.K., "Drained Tension Tests on London Clay", Geotechnique, Vol. 19 No. 2, PP. 309-313, (1969)

[9] Fang,H.Y., Foundation Engineering Handbook, Van Nostrand Reinhold, (1991)

[10] Owen,D.R.J., and Hinton,E., Finite Elements in Plasticity, Pineridge Press Limited, Swansea, U.K., (1986).